PHYSICAL REVIEW A VOLUME 52, NUMBER 1 JULY 1995

Comparison of quasiclassical and exact dipole moments for bound-free transitions in hydrogen

M. S. Adams,* M. V. Fedorov,† V. P. Krainov,‡ and D. D. Meyerhofer§
Laboratory for Laser Energetics, University of Rochester, 250 East River Road, Rochester, New York 14623-1299

(Received 6 December 1994)

A quasiclassical expression for the bound-free dipole moment in hydrogen is found to be in good agreement with the exact Gordon formula values. The approximation has the advantage of clearly indicating the dependence of the dipole moment on the initial- and final-state parameters. The quasiclassical expression is derived for small angular momentum states. The lowest-order angular momentum correction is required for good agreement in the visible frequency range. This correction term scales as $\omega(l+1)^3$ rather than $\omega(l+\frac{1}{2})^3$ as might be expected for the Langer modification.

PACS number(s): 32.70.Cs, 03.65.Sq, 32.80.Cy

I. INTRODUCTION

The dipole moment for a single-photon, bound-bound, bound-free, or free-free transition in hydrogen was explicitly evaluated by Gordon in 1929 [1]. These results have become known as the Gordon formulas. While the Gordon formulas have the advantage of being exact, they are not transparent. The quasiclassical approximation has been used to understand the dependence of the dipole moment on the initial energy, angular momentum, and photon frequency involved in the transition [2,3]. Trippenbach *et al.* used this approach to approximate both bound-bound and free-free transitions and compared them to the exact values [3]. Goreslavskii, Delone, and Krainov applied this approximation to bound-bound, bound-free, and free-free transitions [4,5]. These results have been used to gain insight into such areas as stabilization of atoms in intense fields [6–8] ionization from coherently populated Rydberg levels [6], and strong-field ionization [7].

This paper analyzes a simplification of the quasiclassical expression for bound-free transitions. A first-order correction in angular momentum is derived and shown to be necessary even for zero angular momentum states. This correction extends the usefulness of the approximation into the visible and infrared spectral regions.

Section II presents a quasiclassical approach to calculating the dipole moment. This is performed by using quasiclassical wave functions and assembling the matrix element from them. In Sec. III an evaluation of the quasiclassical approach is given by comparing its predictions to the exact values given by the Gordon formula. Finally, in the Appendix, approximations that delineate the quasiclassical regime are used to expand the bound-bound Gordon formula. The result is then analytically continued to give the bound-free approximation to the dipole moment and is in good agreement with that calculated in Sec. II.

II. QUASICLASSICAL DERIVATION

The quasiclassical approximation incorporates aspects of both classical and quantum mechanics. In this approximation, the electron is treated as having a wave function determined by its classical momentum, which in turn is a function of its quantum-mechanical energy [9]. More generally, any approach that has both classical and quantum-mechanical variables is referred to as quasiclassical.

The derivation of the bound-free dipole moment proceeds along much the same lines as that given in Ref. [4]. First the quasiclassical dipole matrix element is assembled by inserting the quasiclassical wave function (in the classically permitted region of motion) given in the WKB approximation [9] as

$$\varphi_{nl}=\left[\frac{2}{\pi n^3}\right]^{1/2}\frac{1}{r\sqrt{p_{nl}}}\cos\left[\int_{r_{nl}}^{r}p_{nl}dr-\frac{\pi}{4}\right] \tag{1}$$

(where $r_{nl}<r<\tilde{r}_{nl}$, and r_{nl} and $\tilde{r}_{nl}$ are the left and right classical turning points) into the dipole matrix element

$$R_{nl}^{ml+1}=\int_0^\infty \varphi_{nl}\varphi_{ml+1}r^3dr\ . \tag{2}$$

Atomic units are used throughout. The quasiclassical momentum is

$$p_{nl}=\sqrt{-1/n^2+2/r-(l+\tfrac{1}{2})^2/r^2}\ .$$

It will be shown below that only the classically permitted region gives a significant contribution to the integral of Eq. (2). It is with this in mind that the integral may be

---

*Permanent address: Laboratory for Laser Energetics and Institute of Optics, University of Rochester, Rochester, NY 14623.

†Permanent address: Russian Academy of Sciences, General Physics Institute, 38 Vavilov Street, 117942 Moscow, Russia.

‡Permanent address: Moscow Institute of Physics and Technology, 141700 Dolgoprudny, Moscow Region, Russia.

§Permanent address: Laboratory for Laser Energetics and Department of Mechanical Engineering, University of Rochester, Rochester, NY 14623.

extended throughout space. Note that the momentum is defined with the Langer modification [9]. The Langer modification replaces the $l(l+1)$ in the momentum by $(l+\frac{1}{2})^2$.

At this point the characteristic approximation of the quasiclassical regime is invoked, i.e., $m,n \gg 1$. This permits the inner turning points in Eq. (2) to be taken as approximately equal. Then the cosines may be combined using the trigonometric identity

$$\cos(A)\cos(B)=\frac{\cos(A-B)+\cos(A+B)}{2} . \tag{3}$$

The matrix element is now given by

$$R_{nl}^{ml+1}=\frac{1}{\sqrt{\pi(nm)^3}}\int_0^\infty \frac{r}{\sqrt{p_{nl}p_{ml+1}}} \times\cos\left[\int_{r_{nl}}^{r}(p_{nl}-p_{ml+1})dr'\right]dr , \tag{4}$$

where the term corresponding to $\cos(A+B)$ has been dropped as the integrand oscillates rapidly.

Approximations to the quasiclassical momentum are required to proceed further. The momentum can be Taylor expanded with $2/r$ taken much larger than the other terms. This approach leads to an estimate of the momentum

$$p_{nl}\approx\left[\frac{2}{r}\right]^{1/2}\left\{1-\frac{r}{4}\left[\frac{+1}{n^2}+\frac{(l+\frac{1}{2})^2}{r^2}\right]\right\} ; \tag{5}$$

thus the difference in momenta is

$$p_{nl}-p_{ml+1}\approx\sqrt{2/r}\,[(l+1)/(2r)-\omega r/2] .$$

Integrating this difference and substituting in Eq. (4) produces

$$R_{nl}^{ml+1}\approx\frac{1}{2\pi(nm)^{3/2}}\left[\int_0^\infty \frac{r}{\sqrt{p_{nl}p_{ml+1}}}\exp\left\{i\left[\frac{2\omega r^{3/2}}{3\sqrt{2}}+\frac{2(l+1)}{\sqrt{2r}}\right]\right\}dr+\text{c.c.}\right] . \tag{6}$$

The most significant region is where the exponential oscillates most slowly and thus contributes most to the integral. The characteristic quasiclassical length, associated with the first term in the exponential, is of the order of $\omega^{-2/3}$, $r_{nl} \ll \omega^{-2/3} \ll \tilde{r}_{nl}$. The second factor in the exponential contributes significantly close to the left turning point for s and p states. For states of higher angular momentum its domain of significance is outside the classically allowed region. The remaining quasiclassical momenta in the preexponential factor in the integrand may be approximated as $2/r$. This is justified by analyzing the integrand at both end points. On the left the integrand vanishes due to the r in the numerator. On the right the exponential oscillates rapidly and averages to zero. Thus the extra terms in these momenta may be neglected.

The final step is to expand part of the exponential in Eq. (6). The exponential term containing $r^{-1/2}$ is expanded in a Taylor series while the other is integrated exactly. The first two terms of this series produce the zero- and first-order approximations to this matrix element as given by

$$R_{nl}^{ml+1}=\frac{0.4108}{(nm)^{3/2}\omega^{5/3}}\left\{1+\frac{\pi}{2}\left[\frac{\omega(l+1)^3}{3}\right]^{1/3}\right\} . \tag{7}$$

It is this result when analytically continued to the bound-free regime that agrees with Eq. (A12) and will be compared with the Gordon formula.

The analytic continuation to the bound-free case requires use of the following prescription:

$$R_{nl}^{El+1}=\frac{R_{nl}^{ml+1}|_{m\to -i/k}}{k^{3/2}\sqrt{1-e^{-2\pi/k}}} , \tag{8}$$

where $|_{m\to -i/k}$ means substitute $-i/k$ for m in R_{nl}^{ml+1}. The factors in the denominator are required to account for the differing normalizations of the bound and free states and thus maintain the continuity of the wave function across the threshold. In the limit $k \ll 1$, this results in removing the factor $m^{3/2}$ and thus produces

$$R_{nl}^{El+1}=\frac{0.4108}{n^{3/2}\omega^{5/3}}\left\{1+\frac{\pi}{2}\left[\frac{\omega(l+1)^3}{3}\right]^{1/3}\right\} . \tag{9}$$

In the Appendix the bound-free matrix element is derived by an expansion of the Gordon formula [3–5] [see Eqs. (A11) and (A12)]. Equations (A11) and (A12) agree with Eqs. (7) and (9) in the limit $\omega(l+1)^3 \ll 0.77$.

It should be noted that an expansion of Eq. (8) in Ref. [4] will produce a different correction term. (In addition, there is an extra factor of $p^{3/2}$ in the same equation that must be divided out to correctly account for the differing normalization of the two types of states involved in the transition.) That term will scale as $(\omega l^3)^{1/3}$ and will therefore agree with Eq. (7) of this paper only in the limit $l \gg 1$. The correction term is $l+1$ because one unit of angular momentum is exchanged in a dipole transition. If the difference $p_{nl}-p_{ml+a}$ is calculated, the resulting correction term scales as $l+(a^2+a)/2$ and will thus be different for different order transitions.

III. ANALYSIS

In this section the quasiclassical approximation [i.e., Eq. (9)] is compared to the Gordon formula. Our calculations of the exact matrix elements were in agreement with several others [10–12].

In Fig. 1, the ratio of the Gordon formula for a bound s state to a p state at threshold [i.e., $\omega=1/(2n^2)$] to the quantities $1/n^{3/2}\omega^{5/3}$ and $[1+(\pi/2)\omega^{1/3}]/n^{3/2}\omega^{5/3}$ [see

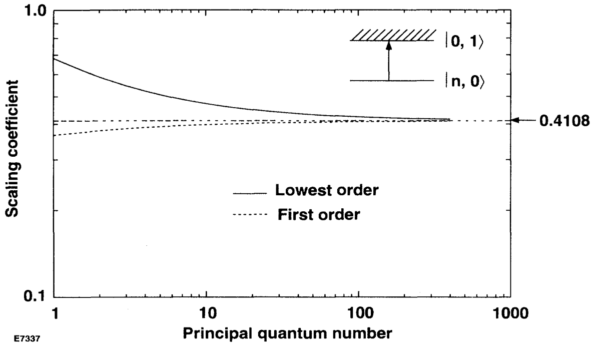

FIG. 1. The ratio of quasiclassical (qc) approximations $1/n^{3/2}\omega^{5/3}$ and $[1+(\pi/2)\omega^{1/3}]/n^{3/2}\omega^{5/2}$ to the exact Gordon formula value for a bound s state to a p state at threshold is plotted as a function of bound-state principal quantum number.

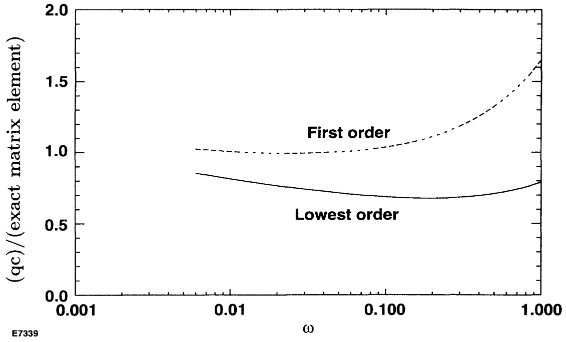

FIG. 3. The same ratios as in Fig. 1 are plotted as a function of frequency for the initial state $n=10$, $l=0$.

Eq. (9)] is plotted as a function of the bound-state principal quantum number. This ratio is defined as the scaling coefficient [i.e., the value 0.4108 in Eq. (9)]. From Fig. 1 it should be noted that even for an s state (which according to Ref. [4] would have no higher-order corrections) the correction presented here improves the accuracy of the approximation. The quasiclassical approximation is expected to be inapplicable to low-lying bound states (i.e., $n \approx 1$) because the condition that the difference between the turning points be negligible will break down. Indeed, the figure shows that the quasiclassical approximation improves significantly as n increases. In addition, whereas the lowest-order estimate requires $n \sim 20$ to be accurate to 10%, when the correction term is included in Eq. (9) the result is in good agreement for initial states as low as $n=2$. Finally, when $n \geq 50$, the first-order approximation is essentially indistinguishable from the exact result. It is not until $n \geq 200$ that the lowest-order estimate attains the same accuracy.

The ratio of the quasiclassical to the exact matrix element as a function of frequency is plotted in Fig. 2 for $n=100$. As ω increases, the lowest-order approximation [i.e., Eq. (A12)] deviates strongly from the exact result. This corresponds to the final bound state no longer being much higher than the initial state in the bound-bound approximation. The first-order correction term [i.e., Eq. (9)] delays this divergence across four orders of magnitude of frequency. Not until the radiation inducing the transition is in the near ultraviolet does the accuracy of the approximation begin to decrease.

The same ratio as Fig. 2 is plotted versus frequency in Fig. 3 for $n=10$. Again the lowest-order approximation begins to break down very close to threshold. The first-order contribution extends this regime of applicability by at least an order of magnitude across the frequency spectrum. Recall that lowest-order behavior dominates when $\omega(l+1)^3 \ll 0.77$. Indeed, for frequencies satisfying this condition in Figs. 2 and 3 (i.e., near threshold) the lowest-order and first-order curves are approaching one another. For higher frequencies only the approximation including the first-order correction is valid.

All the transitions discussed to this point have been s to p (i.e., $l=0$ to $l=1$). The modulus of the dipole matrix element including the first-order correction is plotted as a function of frequency in Fig. 4. This is done for $n=60$ and p-to-d and d-to-f transitions. If the first-order correction were neglected in these cases, the quasiclassical approximation would be severely restricted. This is due to the fact that the correction scales as the $(l+1)^3$. For example, for the $l=1 \rightarrow 2$ transition the region of lowest-order behavior would correspond to $0.000\,14 \leq \omega \ll 0.029$, which spans only two orders of magnitude. Since the principal quantum numbers con-

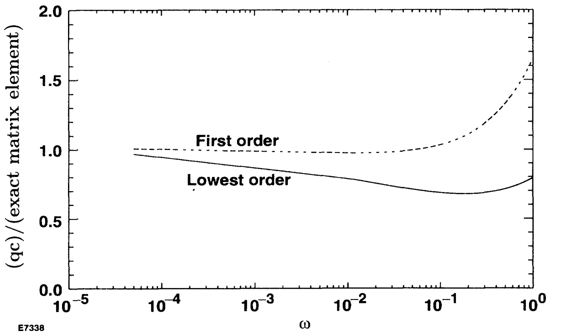

FIG. 2. The same ratios as in Fig. 1 are plotted as a function of frequency for the initial state $n=100$, $l=0$.

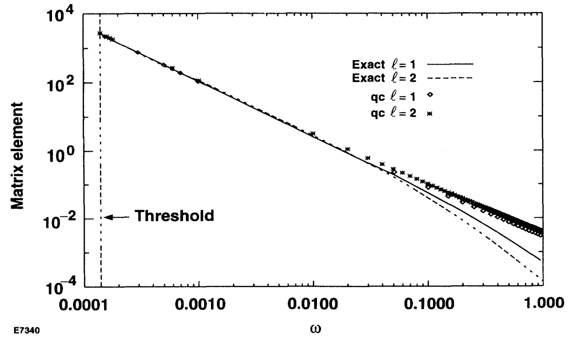

FIG. 4. The exact matrix element is plotted along with the first-order quasiclassical expression for $n=60$ and $l=1,2$.

sidered here allow for very high angular momentum states, the usefulness of the lowest-order approximation will severely degrade.

Near threshold the exact values and the first-order quasiclassical approximation are in excellent agreement. In fact, the region of agreement extends over at least three orders of magnitude (at least a full decade over the lowest-order approximation). In addition, the second-order correction term is negative and so would further extend the range of the approximation.

Experimentally the photoionization cross section $\sigma_1^{(nl)}$ was measured recently by Beterov and Fateev [13] for Rydberg p states ($l=1$ and $n=12-19$) of sodium atoms. Using the quantum defect, the quasiclassical theoretical cross section was shown to be twice the experimentally measured one at the threshold ($n=n_0=12$). Close to threshold (at $n>n_0$ and approaching $n=19$), however, the measured and quasiclassical cross sections agree. Then as a function of n the exact photoionization cross section approaches its asymptotic value given by Eq. (9).

IV. CONCLUSIONS

The quasiclassical approximation to the bound-free dipole matrix element in hydrogen provides a useful means of understanding the behavior of this quantity with respect to the initial and final states of the transition. This in turn allows deeper understanding of the behavior of atoms in the radiation field due to the transparency of this simplification. An extension of this approximation allows excellent estimation of exact dipole moments over a range of parameters accessible to current experiments while clearly expressing the behavior of the dipole moment with respect to the relevant variables.

ACKNOWLEDGMENTS

The authors wish to thank R. Grobe and M. Y. Ivanov for useful comments. This work was supported by the National Science Foundation Contract No. PHY9304335 and the U.S. Department of Energy Office of Inertial Confinement Fusion under Cooperative Agreement No. DE-FC03-92SF19460, the University of Rochester, and the New York State Energy Research and Development Authority.

APPENDIX: DERIVATION FROM THE GORDON FORMULA

The derivation of the quasiclassical result from the exact Gordon formula is presented for the sake of completeness. The derivation of Eqs. (A11) and (A12) from quasiclassical theory is well known [3–5]. These results have not, however, been presented as a limiting case of the exact one. This derivation should serve as an aid in illustrating the approximations inherent in the quasiclassical formulation. The Gordon formula in Eq. (A1) gives the exact value of the radial part of the bound-bound dipole moment in hydrogen and is represented for a transition from $|n,l\rangle$ to $|ml+1\rangle$ as [1,14]

$$R_{nl}^{ml+1}=\frac{(-1)^{n-l-1}}{4(2l+1)!}\frac{\sqrt{(m+l+1)!(n+l)!}}{\sqrt{(m-l-2)!(n-l-1)!}}(4nm)^{l+2}\frac{(m-n)^{m+n-2l-4}}{(m+n)^{m+n}}$$
$$\times\left\{{}_2F_1\left[-(m-l-2),(n-l-1),2l+2;\ \frac{-4nm}{(m-n)^2}\right]\right.$$
$$\left.-\left[\frac{m-n}{m+n}\right]^2{}_2F_1\left[-(m-l),(n-l-1),2l+2;\ \frac{-4mn}{(m-n)^2}\right]\right\}. \tag{A1}$$

Equation (A1) may be simplified by considering the regime where $m \gg n \gg 1$, $n \gg l$ and applying the confluence relation [2]

$$\lim_{\beta\to\infty}{}_2F_1(-a,\alpha+1+\beta+a,\alpha+1;\ x)=M(-a,\alpha+1;\ \beta x)\ , \tag{A2}$$

where ${}_2F_1$ and M are the general and confluent hypergeometric functions, respectively. The difference of hypergeometric functions in Eq. (A1) (denoted hereafter as Δ) then reduces to

$$\Delta=\left\{M\left[-(m-l),2l+2,\frac{4mn(m+n-1)}{(m-n)^2}\right]\right.$$
$$-\left[\frac{m-n}{m+n}\right]^2$$
$$\left.\times M\left[-(m-l),2l+2,\frac{4mn(m+n+1)}{(m-n)^2}\right]\right\}. \tag{A3}$$

This may be modified by Taylor-expanding each confluent hypergeometric function as

$$M(a,b,x+\varepsilon)\approx M(a,b,x)+\varepsilon M'(a,b,x)\ , \tag{A4}$$

where the prime denotes differentiation with respect to x. The first confluent hypergeometric function becomes

$$\begin{aligned} M&\left[-(m-l),2l+2,\frac{4mn(m+n-1)}{(m-n)^2}\right]\\ &\approx M\left[-(m-l),2l+2,\frac{4mn(m+n)}{(m-n)^2}\right]\\ &\quad-\varepsilon M'\left[-(m-l),2l+2,\frac{4mn}{(m-n)^2}\right]\ , \end{aligned}\tag{A5}$$

while the second may be approximated as

$$\begin{aligned} M&\left[-(m-l),2l+2,\frac{4mn(m+n+1)}{(m-n)^2}\right]\\ &\approx M\left[-(m-l),2l+2,\frac{4mn(m+n)}{(m-n)^2}\right]\\ &\quad+\varepsilon M'\left[-(m-l),2l+2,\frac{4mn(m+n)}{(m-n)^2}\right] \end{aligned}\tag{A6}$$

with

$$\varepsilon=\frac{m}{(m-n)^2}\ .$$

Then Δ may be rewritten, assuming $(m-n)^2/(m+n)^2\approx 1$,

$$\begin{aligned} \Delta=\varepsilon&\left\{M\left[-(m-l),2l+2,\frac{4mn(m+n)}{(m-n)^2}\right]\right.\\ &\left.-2M'\left[-(m-l),2l+2,\frac{4mn(m+n)}{(m-n)^2}\right]\right\}\ . \end{aligned}\tag{A7}$$

Employing Eq. 13.5.21 from Ref. [15], M can be expanded, for large a, b, and x,

$$M(a,b,x)\approx e^{x/2}(b-2a)^{2/3-b}\Gamma(b)(-1)^a\mathrm{Ai}(t)\ , \tag{A8}$$

where

$$t=(b-2a)^{2/3}\left[\frac{x}{2(b-2a)}-1\right]\ . \tag{A9}$$

$\Gamma(x)$ is the gamma function and $\mathrm{Ai}(t)$ is the Airy function. If the derivative with respect to x is taken in Eq. (A8), an approximation may be developed for M':

$$\begin{aligned} M'(a,b,x)\approx{}&\tfrac{1}{2}M(a,b,x)+e^{x/2}(b-2a)^{2/3-b}\Gamma(b)\\ &\times(-1)^a\left[\frac{d\mathrm{Ai}(t)}{dx}\right]\ . \end{aligned}\tag{A10}$$

The factorials may be expressed as simple powers [e.g., $(n+l)!\approx n^{n+l}$], and the standard limit definition of e^x can be used. The Gordon formula may then be reduced to [6]

$$R_{nl}^{ml+1}=\frac{0.4108}{\omega^{5/2}(nm)^{3/2}}\ . \tag{A11}$$

These results may be analytically extended to the bound-free case [see Eqs. (7)–(9)], which results in the removal of the m dependence (if $k\ll 1$) and is represented by [4]

$$R_{nl}^{El+1}=\frac{0.4108}{\omega^{5/3}n^{3/2}}\ . \tag{A12}$$

It should be noted that, since the final principal quantum number was taken to be very large (i.e., $m\gg 1$) in the derivation of Eq. (A11), its analytical continuation should be valid for free states relatively close to threshold.

[1] W. Gordon, Ann. Phys. (Leipzig) **2**, 1031 (1929).

[2] L. D. Landau and E. M. Lifshitz, *Quantum Mechanics: Non-Relativistic Theory,* 3rd ed. (Pergamon, New York, 1977).

[3] M. Trippenbach, K. Rzazewski, M. V. Fedorov, and A. E. Kazakov, J. Phys. B **22**, 1193 (1989).

[4] S. P. Goreslavskii, N. B. Delone, and V. P. Krainov, Zh. Eksp. Teor. Fiz. **82**, 1789 (1982) [Sov. Phys. JETP **55**, 1032 (1982)].

[5] N. B. Delone, S. P. Goreslavsky, and V. P. Krainov, J. Phys. B **22**, 2941 (1989).

[6] M. V. Federov and A. M. Movsesian, J. Opt. Soc. Am. **5**, 850 (1988).

[7] J. Peatross, M. V. Fedorov, and D. D. Meyerhofer, J. Opt. Soc. Am. B **9**, 1234 (1992).

[8] A. E. Kazakov, V. P. Makarov, and M. V. Fedorov, Zh. Eksp. Teor. Fiz. **70**, 38 (1976).

[9] N. Fröman and P. O. Fröman, *JWKB Approximation: Contributions to the Theory* (North-Holland, Amsterdam, 1965).

[10] H. B. Bebb, J. Math. Phys. **7**, 955 (1966).

[11] A. Burgess, Mem. R. Astron. Soc. **69**, 1 (1964).

[12] K. Omidvar and P. T. Guimaraes, Astrophys. J. Suppl. Ser. **73**, 555 (1990).

[13] I. M. Beterov and N. Fateev (unpublished).

[14] H. A. Bethe and E. E. Salpeter, *Quantum Mechanics of One- and Two-Electron Atoms,* 2nd ed. (Plenum/Rosetta, New York, 1977).

[15] *Handbook of Mathematical Functions with Formulas, Graphs, and Mathematical Tables,* Natl. Bur. Stand. Appl. Math. Ser. No. 55, edited by M. Abramowitz and I. A. Stegun (U.S. GPO, Washington, D.C., 1964).